Journal for ImmunoTherapy of Cancer

hMENA isoforms regulate cancer intrinsic type I IFN signaling and extrinsic mechanisms of resistance to immune checkpoint blockade in NSCLC

Paola Trono,[1,2] Annalisa Tocci,[1] Belinda Palermo,[1] Anna Di Carlo,[1] Lorenzo D'Ambrosio ,[1] Daniel D'Andrea,[3] Francesca Di Modugno,[1] Francesca De Nicola,[4] Frauke Goeman,[4] Giacomo Corleone,[4] Sarah Warren ,[5] Francesca Paolini,[1] Mariangela Panetta,[1] Isabella Sperduti,[6] Silvia Baldari,[1] Paolo Visca,[7] Silvia Carpano,[8] Federico Cappuzzo,[8] Vincenzo Russo,[9] Claudio Tripodo,[10] Paolo Zucali,[11] Vanesa Gregorc,[9] Federica Marchesi ,[12,13] Paola Nistico [1]

To cite: Trono P, Tocci A, Palermo B, *et al*. hMENA isoforms regulate cancer intrinsic type I IFN signaling and extrinsic mechanisms of resistance to immune checkpoint blockade in NSCLC. *Journal for ImmunoTherapy of Cancer* 2023;**11**:e006913. doi:10.1136/jitc-2023-006913

► Additional supplemental material is published online only. To view, please visit the journal online (http://dx.doi.org/10.1136/jitc-2023-006913).

PT and AT are joint first authors.

Accepted 08 August 2023

For numbered affiliations see end of article.

Correspondence to
Dr Paola Nistico;
paola.nistico@ifo.it

Dr Paola Trono;
paola.trono@cnr.it

ABSTRACT

Background Understanding how cancer signaling pathways promote an immunosuppressive program which sustains acquired or primary resistance to immune checkpoint blockade (ICB) is a crucial step in improving immunotherapy efficacy. Among the pathways that can affect ICB response is the interferon (IFN) pathway that may be both detrimental and beneficial. The immune sensor retinoic acid-inducible gene I (RIG-I) induces IFN activation and secretion and is activated by actin cytoskeleton disturbance. The actin cytoskeleton regulatory protein hMENA, along with its isoforms, is a key signaling hub in different solid tumors, and recently its role as a regulator of transcription of genes encoding immunomodulatory secretory proteins has been proposed. When hMENA is expressed in tumor cells with low levels of the epithelial specific hMENA^{11a} isoform, identifies non-small cell lung cancer (NSCLC) patients with poor prognosis. Aim was to identify cancer intrinsic and extrinsic pathways regulated by hMENA^{11a} downregulation as determinants of ICB response in NSCLC. Here, we present a potential novel mechanism of ICB resistance driven by hMENA^{11a} downregulation.

Methods Effects of hMENA^{11a} downregulation were tested by RNA-Seq, ATAC-Seq, flow cytometry and biochemical assays. ICB-treated patient tumor tissues were profiled by Nanostring IO 360 Panel enriched with hMENA custom probes. OAK and POPLAR datasets were used to validate our discovery cohort.

Results Transcriptomic and biochemical analyses demonstrated that the depletion of hMENA^{11a} induces IFN pathway activation, the production of different inflammatory mediators including IFNβ *via* RIG-I, sustains the increase of tumor PD-L1 levels and activates a paracrine loop between tumor cells and a unique macrophage subset favoring an epithelial-mesenchymal transition (EMT). Notably, when we translated our results in a clinical setting of NSCLC ICB-treated patients, transcriptomic analysis revealed that low expression of hMENA^{11a}, high expression of IFN target genes and high macrophage score identify patients resistant to ICB therapy.

Conclusions Collectively, these data establish a new function for the actin cytoskeleton regulator hMENA^{11a} in modulating cancer cell intrinsic type I IFN signaling and extrinsic mechanisms that promote protumoral macrophages and favor EMT. These data highlight the role of actin cytoskeleton disturbance in activating immune suppressive pathways that may be involved in resistance to ICB in NSCLC.

WHAT IS ALREADY KNOWN ON THIS TOPIC

⇒ The epithelial hMENA^{11a} isoform when downregulated triggers a partial epithelial-mesenchymal transition and identifies non-small cell lung cancer (NSCLC) patients with poor prognosis.

⇒ Immune checkpoint blockade (ICB) has achieved remarkable success in NSCLC treatment although major challenges still remain for broadening patients benefit.

WHAT THIS STUDY ADDS

⇒ Here, we used multiple methodologies to define how the disturbance of actin cytoskeleton related to hMENA^{11a} downregulation induces type I IFN secretion and PD-L1 expression in tumor cells via RIG-I and activates a detrimental paracrine loop between tumor cells and macrophages.

HOW THIS STUDY MIGHT AFFECT RESEARCH, PRACTICE OR POLICY

⇒ Our findings identify key features that may characterize tumors responsive or not to ICB treatment and demonstrate how the cancer cell actin cytoskeleton disturbance may influence immune-related pathways and in turn ICB efficacy.

BACKGROUND

Immunotherapy has determined remarkable advances in the management of non-small cell lung cancer (NSCLC). However, rates of relapse after immune checkpoint blockade (ICB) are high among patients with

lung cancer.[1] Thus, the understanding of mechanisms underlying resistance to therapy and the identification of molecular determinants and biomarkers to guide patient selection represent an urgency for this still deadly disease. The phenotype of tumor microenvironment (TME), including T and B cells organized in tertiary lymphoid structures, has been linked to clinical response, although only programmed death-ligand 1 (PD-L1) status drives the selection of patients to be treated with ICB.[2]

Type I IFNs have been largely involved in antitumor immunity,[3] although the advance in the field highlighted a divergent impact in both cancer development and resistance to therapy.[4–9] Indeed type I IFNs may sustain both cancer intrinsic and extrinsic suppressive networks responsible of the failure of the anticancer therapies, including ICB.[10–12]

Among the immunosuppressive networks, epithelial-mesenchymal transition (EMT) has been identified as a crucial program that deregulates tissue architecture[13] and leads to functional changes in cell migration and invasion, through cytoskeleton reorganization.[14] Noteworthy EMT favors an immune suppressive TME, fundamental for therapy resistance.[15 16]

EMT also relies on a defined alternative spliced transcriptome[17] critical in shaping the process with central coordinators such as epithelial splicing regulatory proteins 1 and 2 (ESRP1 and ESRP2). Among the ESRP1-2 regulated genes, *ENAH*,[18] codes for the actin binding protein hMENA that belongs to ENA/VASP family.[19] We have reported two tissue-specific isoforms, the epithelial hMENA^{11a} and the mesenchymal hMENAΔv6[20] which differently contribute to cancer progression and associate to patient prognosis, with hMENA^{11a} identifying pancreatic ductal adenocarcinoma (PDAC) and NSCLC patients with better prognosis.[21–23] The epithelial-associated isoform hMENA^{11a} sustains cell-cell junction integrity in epithelial tumors[22] where its expression is regulated by ESRP1-2. Differently TGFβ, the master regulator of EMT and of an immunosuppressive TME,[24] downregulates both ESRP and hMENA^{11a}.[22 25]

All the actin cytoskeleton dynamics also occurring during EMT are sensed by the immune system, as recently reported for RIG-I-like receptor (RLR)-mediated innate immunity.[26] Indeed, the innate viral nucleotide sensor retinoic acid-inducible gene-I (RIG-I) protein is associated with the actin cytoskeleton in epithelial cancer cells, where actin depolymerization is sufficient to induce RIG-I activation and in turn IFNβ secretion.[27]

Here, we found a novel role of the actin binding isoform hMENA^{11a} that, when downregulated as occurs in EMT, activates type I IFN signaling by regulating the immune sensor RIG-I. We observed that the depletion of hMENA^{11a} in tumor cells induces the production of different inflammatory mediators such as IL6, IL8, CXCL1 and increases the expression of RIG-I which is responsible of IFNβ secretion and of programmed death-ligand 1 PD-L1 expression in tumor cells. Notably, we found that the absence of hMENA^{11a} activates a paracrine loop between tumor cells and macrophages which acquire a peculiar phenotype sustained by IFN-I signaling. These macrophages in turn secrete factors which favor an EMT phenotype. Of clinical relevance the low expression of hMENA^{11a}, high expression of IFN target genes and high macrophage score identify non-responding NSCLC-ICB-treated patients.

Based on these evidences, we propose a new mechanism of resistance that, starting from actin cytoskeleton modification, determines an increased expression of the immune sensor RIG-I, IFNβ, PD-L1 in tumor cells and may contribute to an immune suppressive TME. The validation of our results in a large cohort of patients will bring to the forefront the possibility of employing this signature in stratifying ICB non-responder or responder NSCLC patients.

MATERIALS AND METHODS

Cell lines

Human NSCLC cell lines were purchased from American Type Culture Collection, and cultured in RPMI 1640 Medium, supplemented with 10% fetal bovine serum (FBS), 1% (vol/vol) penicillin-streptomycin antibiotics and 1% (vol/vol) L-glutamine. Cell lines were grown at 37°C. All cell lines were routinely tested for Mycoplasma (Mycoplasma PCR Reagent set, Euroclone) and authenticated by short tandem repeat (STR) profiling (BMR Genomics, Italy). Mutational status of NSCLC cell lines is reported in online supplemental table 1.

Purification and culture of macrophages

Human peripheral blood mononuclear cells were isolated from healthy donor buffy coats or peripheral blood samples by Lympholite-H (#CL5020, Euroclone). Buffy coats were provided by the Immunohematology and Transfusional Medicine Unit of Regina Elena National Cancer Institute. Monocytes were purified by anti-CD14 microbeads (#130-050-201, MiltenyiBiotec) according to the manufacturer's instructions. Purified CD14+ monocytes were incubated for 7 days in RPMI 1640 supplemented with 10% inactivated FBS and 50 ng/mL macrophage colony-stimulating factor (M-CSF, #300-25, Peprotech) to derive monocyte-derived macrophages (M0-macrophages). M0-macrophages were treated for 24 hours with conditioned medium (CM) from NSCLC cell lines diluted in RPMI (CM:RPMI 2:1). M0-macrophages were treated with IFNβ for 24 hours or preincubated with anti-Interferon-α/β Receptor Chain 2 for 48 hours before adding CM. Cells were harvested using EDTA 5 mmol for analysis.

Patients and gene expression analysis using Nanostring Technology

Patients with histologically confirmed NSCLC who received nivolumab or pembrolizumab treatment at Regina Elena National Cancer Institute in Rome (IRE), Humanitas Research Hospital in Rozzano (HUM) and

San Raffaele Hospital in Milan (HSR) were enrolled. Patient consent and ethics approval were obtained. Fifteen patients, whose tumors were available, were selected and their clinical pathological characteristics are shown in online supplemental table 2. Patients were classified as good responders (GRs) in absence of disease progression at 10 months from the treatment, poor responders (PRs) in case of disease progression at 3 months.

RNA was extracted from 5 µm FFPE sections of tumor tissues collected at the time of diagnosis with AllPrep DNA/RNA FFPE kit (Qiagen). The quantity and purity of the RNA were assessed with the NanoDrop spectrophotometer. The quality of the RNA was controlled with the Bioanalyzer employing the Agilent RNA 6000 Pico or Nano Kit (Agilent Technologies, Santa Clara, California, USA). Gene expression was measured using the Nanostring nCounter PanCancer IO 360 Panel—in collaboration with Nanostring (Seattle, Washington, USA). As input, 100 ng total RNAs were used following the manufacturer's instructions. After the codeset hybridization samples were washed and loaded on the cartridge within the Prep Station and analyzed with the nCounter Digital Analyzer. Along with the 750 genes of the Nanostring nCounter PanCancer IO 360 Panel, custom probes for different splicing variants of the *ENAH* gene (ENAH-a=hMENA^{11a}, ENAH-b=hMENAΔv6, ENAH-c=hMENA+hMENAΔv6) were also included in the analysis of NSCLC tissues.

Statistical analysis

For in vitro experiments, data are expressed as the mean±SEM of at least three different experiments. Data were analyzed either by Microsoft Excel (Microsoft, Redmond, Washington, USA) or GraphPad Prism V.9 (V.9.4.0, GraphPad Software, San Diego, California, USA). Statistical significance was determined by either Student's t-test (normally distributed paired or unpaired dataset) or repeated measure analysis of variance, as indicated in the figure legends. For comparison between matched healthy donor (HD) samples, Wilcoxon U-test, with Bonferroni correction for multiple comparisons, was used. Statistical significance was defined as $p<0.05$.

RESULTS

hMENA^{11a} depletion activates type I IFN pathways and increases PD-L1 expression in NSCLC cell lines

hMENA isoform expression pattern has been proposed to be a prognostic factor, with low hMENA^{11a} expression, along with high overall hMENA, identifying early NSCLC patients with poor prognosis.[21 23]

To gain insights into molecular mechanisms accounting for the poor prognostic value of low levels of hMENA^{11a}, we sought to analyze molecular changes resulting from hMENA^{11a} depletion in NSCLC cell lines, by a whole transcriptome analysis by RNA-Seq approach of two lung adenocarcinoma (ADC) cell lines (H1650 and H2030) with an epithelial phenotype and overexpressing hMENA^{11a} isoform.

To this aim, we specifically silenced hMENA^{11a} in these cell lines (hereafter si11a cells) by siRNA approach and compared their transcriptomic profile with the control cells (transfected with non-targeting siRNA, hereafter sictr cells), and with the profile of cells silenced in total hMENA isoforms (obtained by using siRNA targeting all hMENA isoforms, hereafter sihMENA(t) cells) (figure 1A,B). Expression levels of different isoforms in silenced cells are shown in online supplemental figure S1A.

Surprisingly, Gene Ontology term enrichment analysis of RNA-Seq data indicated that a large fraction of genes that changed their expression profile in response to hMENA^{11a} silencing was mainly involved in type I IFN-related pathways and related cellular response, suggesting that, among the upregulated biological processes in si11a cells, the response to Type I IFN was dominant (figure 1A,B). In particular, in both cell lines, si11a cells showed the upregulation of key molecules involved in the antiviral interferon response, such as the IFN-stimulated genes (ISGs) *OAS1, OASL, ISG15, ANKRD17, RNASEL, IRF9*. Notably, *STAT1* the crucial mediator of interferon transcriptional activity was among the upregulated genes in si11a cells compared with sictr cells and sihMENA(t) cells. Of note, STRING network analysis for predicting protein–protein interactions indicated *ISG15* as a central hub node gene in si11a cells (figure 1C).

Validation of RNA-Seq results by RT-PCR in three epithelial cancer cell lines confirmed that specific hMENA^{11a} silencing, but not hMENA(t) silencing, increases ISG mRNA levels (figure 1D and online supplemental figure S1B).

Since RNA-Seq analysis indicated that the specific hMENA^{11a} depletion activates IFN-related pathways resembling a viral defense response, which typically culminates with IFNβ production, we analyzed IFNβ levels in cell CM. We found that, while H1650 and HCC2935 sictr cells secrete barely detectable levels of IFNβ, si11a cells produce relevant amount of this cytokine, indicating that hMENA^{11a} silencing *per se* increases IFNβ secretion (figure 1E and online supplemental figure S1C, left). Noteworthy, cells silenced for total hMENA isoforms do not produce IFNβ. As expected, we found *IFNB1* upregulation also at transcriptional level in si11a cells (figure 1E and online supplemental figure S1C, right). Of note, H1650 sictr cells, as well as sihMENA(t) cells, showed barely detectable levels of IFNα mRNA, and undetectable IFNγ. Neither IFNα nor IFNγ levels were increased by hMENA^{11a} silencing (online supplemental figure S1D).

To mimic a viral infection, able to trigger type I interferon pathway, we treated H1650 cells with polyinosinic acid-polycytidylic acid Poly(I:C), the synthetic dsRNA analog. As a result, hMENA^{11a} expression was reduced in parallel with an increase of STAT1 expression and activation, along with the production of IFNβ (online supplemental figure S1E).

Treatment of a panel of NSCLC cell lines with IFNβ upregulated PD-L1 expression (figure 2A), indicating

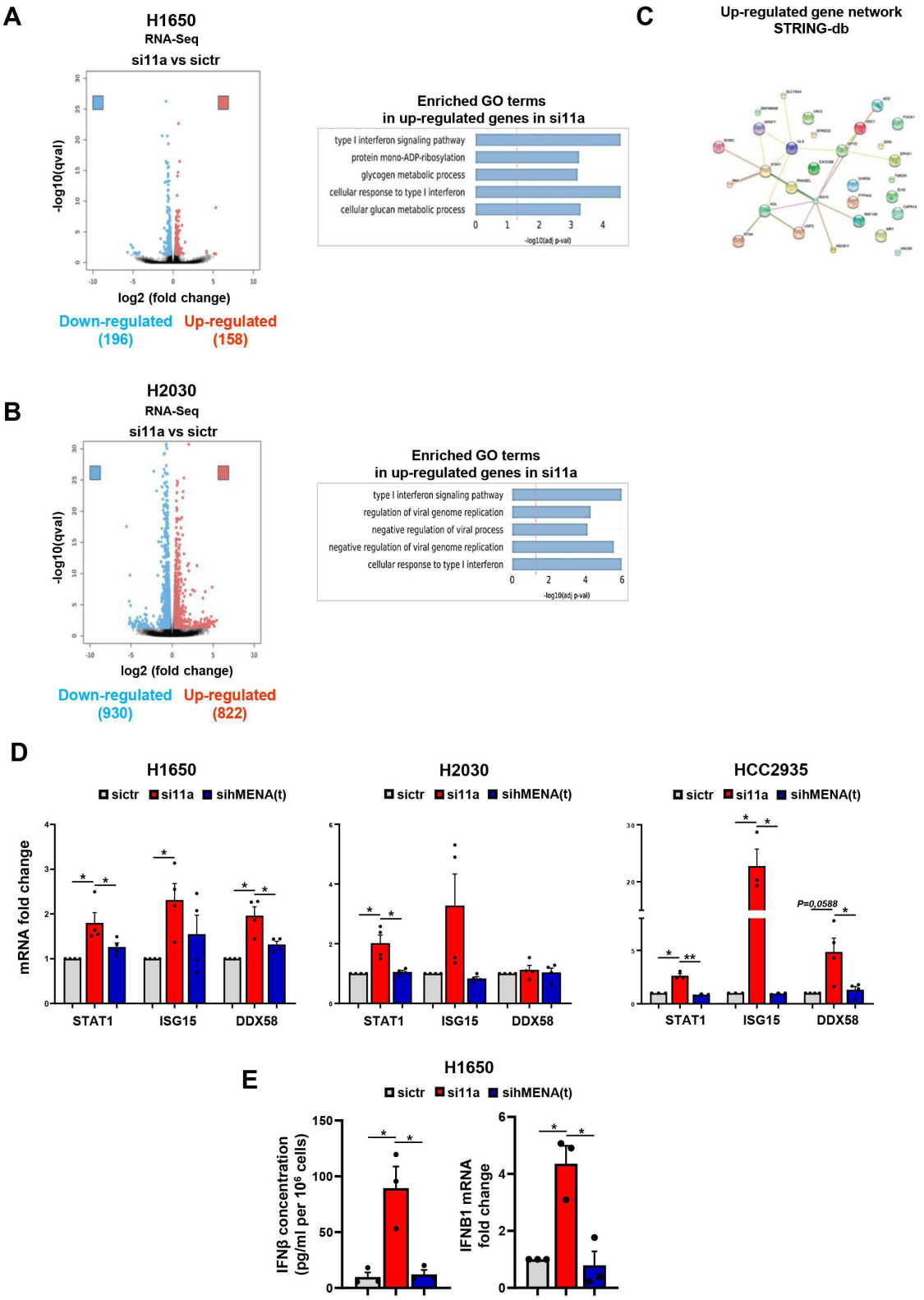

Figure 1 hMENA^{11a} silencing upregulates transcripts of genes related to IFN-signaling pathways in NSCLC cell lines. (A, B) (left) Volcano plot showing statistical significance (qvalue, –log10 scaled) vs fold change (log2 scaled) for genes differentially expressed after deletion of hMENA^{11a} in H1650 and H2030: 196 and 930 downregulated (blue) and 158 and 822 upregulated (red) genes in si11a cells *vs* sictr cells, respectively (q value <0.05). (A, B) (right) Enrichment analyses (GO Biological Process) of upregulated genes in si11a cells, H1650 (up) and H2030 (down). (C) Upregulated gene network in H1650 si11a cells revealed by STRING analysis. (D) qPCR results of mRNA levels of selected genes in sictr, si11a and sihMENA(t) H1650, H2030 and HCC2935 cells. (E) Levels of IFNβ in supernatants evaluated by ELISA (left) and of IFNB1 mRNA by qRT-PCR (*right*) expressed as fold-change relative to control in H1650 sictr, si11a, sihMENA(t) cells. (D, E) P values were calculated by two-tailed Student's t-test. *p≤0.05; **p≤0.01.

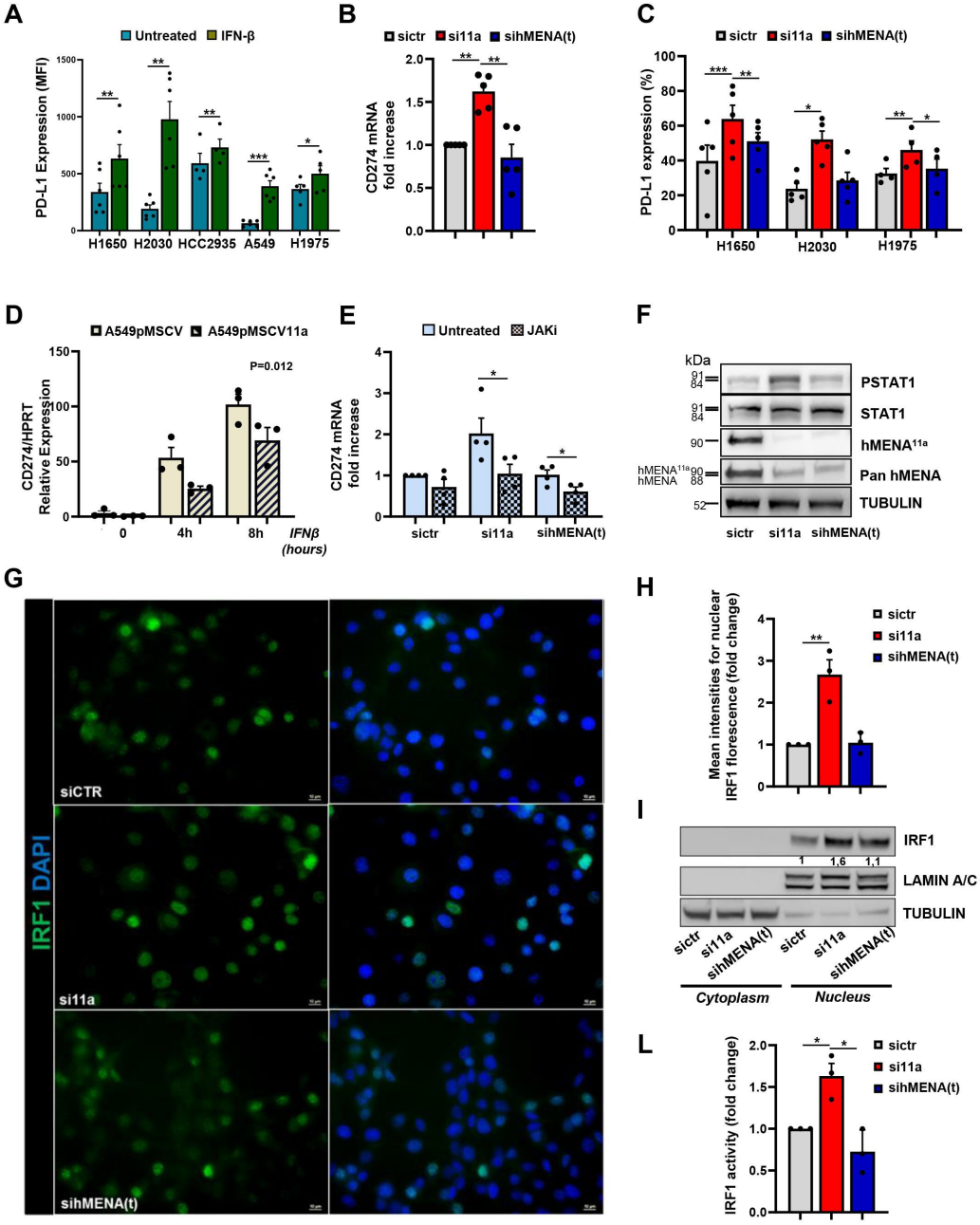

Figure 2 hMENA^{11a} silencing increases PD-L1 at mRNA and protein levels via JAK/STAT1/IRF1 axis in NSCLC cell lines. (A) PD-L1 expression levels (MFI) assessed by flow cytometry analysis in a panel of NSCLC cells, untreated or treated with IFNβ (50 ng/mL) for 24 hours. (B) qRT-PCR results of *CD274* analyzed in sictr, si11a and sihMENA(t) H1650 cells. (C) PD-L1 expression levels assessed by flow cytometry analysis in a panel of sictr, si11a, and sihMENA(t) NSCLC cells. (D) *CD274* mRNA expression levels evaluated by qRT-PCR in A549 transfected with empty vector (pMSCV) or hMENA^{11a} (pMSCV11a), untreated or treated with IFNβ (50 ng/mL) for the indicated hours. (E) qRT-PCR results of *CD274* analyzed in sictr, si11a and sihMENA(t) H1650 cells untreated or treated with JAK inhibitor (5 µM) for 72 hours. (F) Western blotting of cells treated as in (B). (G) Representative images of immunofluorescence of sictr, si11a and sihMENA(t) H1650 stained with anti-IRF1 antibody (green, left panel). Nuclei were stained with DAPI. Scale bar: 10 µm. (H) Quantitative analysis of nuclear IRF1 levels. Mean fluorescent intensities were determined by ImageJ and reported as fold changes. More than 100 cells were counted in three independent experiments. (I) Western blotting of nuclear and cytoplasmic fractions of sictr, si11a and sihMENA(t) H1650 cells. Anti-Lamin A/C and anti-tubulin antibodies were used as nuclear and cytoplasmic markers, respectively. Immunoreactivity was determined by ImageJ and numbers indicate the fold changes of IRF1 *vs* Lamin optical density values. For all western blots, one representative of at least three experiments is reported. (L) Luciferase assays of IRF1 transcriptional reporter activity in sictr, si11a and sihMENA(t) H1650 cells. Cells were cotransfected with non-targeting siRNA (sictr), or hMENA^{11a} specific siRNA (si11a) or siRNA targeting total hMENA (sihMENA(t)) and with inducible IRF1 responsive construct expressing Renilla luciferase. 48 hours later a luciferase assay was performed. Graphs represent mean±SEM of three independent experiments. (A–C, E, H, L). P values were calculated by two-tailed Student's t-test. (D) P value calculated by repeated measure ANOVA. *P≤0.05; **P≤ 0.01; ***P≤0.001. ANOVA, analysis of variance.

that IFNβ is a critical regulator of PD-L1 expression levels in NSCLC cells, as previously reported for IFNγ in melanoma cells.[28]

Given that hMENA^{11a} depletion induced IFNβ production, we investigated whether hMENA^{11a} silencing affects PD-L1 expression. PD-L1 transcript levels increase in NSCLC cell lines after hMENA^{11a} depletion (figure 2B) as well as protein levels, as evidenced by flow cytometry in si11a cells (figure 2C). It is noteworthy that the overexpression of hMENA^{11a} in A549, expressing low basal levels of PD-L1, counteracts PD-L1 increase mediated by IFNβ treatment (figure 2D and online supplemental figure S2A).

To be noticed, ATAC-Seq analysis revealed the existence of an open chromatin region in the *CD274* locus in H1650 si11a cells, further supporting a key role of hMENA^{11a} in the regulation of PD-L1 expression (online supplemental figure S2B). This evidence warrants further investigation in future studies.

Then, to identify paracrine mechanisms of hMENA^{11a}-mediated PD-L1 regulation, we treated the NSCLC cell line H1299, not expressing hMENA^{11a} (online supplemental figure S2C), with the CM of H1650 cells, silenced or not (online supplemental figure S2D), and looked at STAT1 activation, considering its role in IFN-mediated PD-L1 regulation.[28] We observed that only the si11a cell-derived CM, but not sictr nor sihMENA(t), activates STAT1, as revealed by the increased phosphorylation in tyrosine 701, indicative of IFN pathway activation in the recipient H1299 cell line (online supplemental figure S2E). Importantly, in parallel we observed an increase of PD-L1, as detected by flow cytometry (online supplemental figure S2F) thus indicating that si11a cell-derived CM is able to induce activation of IFN pathway and to upregulate PD-L1 expression levels in a paracrine fashion.

Overall, these data show that hMENA^{11a} silencing *per se* activates IFN-related pathways, triggering a viral response program that culminates with IFNβ production and in turn PD-L1 upregulation.

hMENA^{11a} silencing increases PD-L1 at mRNA and protein levels via activation of JAK/STAT1 pathway in NSCLC cell lines

Interferon regulatory factor-1 (IRF1) is a key PD-L1 transcription factor,[28] thus we investigated whether the PD-L1 expression mediated by hMENA^{11a} silencing may be linked to IRF1 activity, which is downstream to IFN/STAT/JAK axis.

To assess the involvement of JAK/STAT1 axis in PD-L1 increase induced by hMENA^{11a} silencing, we used an ATP-competitive JAK inhibitor. The inhibitor completely suppressed STAT1 activation induced by hMENA^{11a} silencing (online supplemental figure S2G) and significantly counteracted PD-L1 mRNA upregulation (figure 2E), clearly indicating that JAK/STAT1 activation participates in PD-L1 increase.

Moreover, we revealed that the depletion of hMENA^{11a} upregulates STAT1 phosphorylation in all tested NSCLC cell lines (figure 2F and online supplemental figure S2H), indicative of the activation of JAK/STAT1 pathway.

To gain deeper insight into the mechanism underlying PD-L1 increase, we analyzed intracellular localization of IRF1, the positive regulator of PD-L1 transcription.[29] Immunoflorescence analysis revealed that IRF1 localizes in both nuclear and cytoplasmic compartments of sictr H1650 cells. Differently its nuclear localization appeared strongly increased in si11a cells, while sihMENA(t) cells showed IRF1 localization comparable to that observed in sictr cells (figure 2G,H). Accordingly, immunoblotting analysis indicated that nuclear localization of IRF1 increases in si11a cells (figure 2I). This was confirmed by evaluating luciferase activity in an inducible IRF1 responsive reporter assay, where we found higher IRF1 activity in cells depleted of hMENA^{11a}, compared with sictr and sihMENA(t) cells (figure 2L). Collectively, these data indicate that hMENA^{11a} affects IRF1 subcellular localization and transcriptional activity, modulates JAK/STAT1/IRF1 signaling pathway and in turn PD-L1 expression.

hMENA^{11a} depletion perturbs cell–cell junction integrity, activates NF-kB pathway, induces proinflammatory cytokines but differs from E-cadherin loss for Type I IFN pathway activation

hMENA^{11a} is expressed in tumor cells with epithelial phenotype and correlates with E-cadherin expression in breast, lung and pancreatic cancers.[20–22] On the other hand, hMENA^{11a} silencing downregulates E-cadherin expression, weakening cell–cell adhesion.[22]

Accordingly, in the current study, we find a significant downregulation of *CDH1* transcripts in H1650 si11a cells, compared with sictr and sihMENA cells (online supplemental figure S3A, left). The decrease of E-cadherin expression in si11a but not in sihMENA(t) cells also occurred at the protein level (online supplemental figure S3A, right) and was accompanied by a critical delocalization of E-cadherin from cell–cell junctions, as observed by confocal analysis (figure 3A, upper panel).

Furthermore, hMENA^{11a} silencing, along with a critically disorganization of F-actin, induces an important delocalization of zonula occludens-1 (ZO-1) at cell junctions, in contrast with the typical honeycomb membrane staining of ZO-1 in sictr cells (figure 3A, lower panel).

Cell–cell junction perturbation has been associated with the activation of NF-kB-driven inflammatory pathways in different tumors[30 31] and accordingly, we found that hMENA^{11a} silencing robustly induces transcripts relative to NF-kB-dependent inflammatory cytokines such as IL6, IL8 and CXCL1 (online supplemental figure S3B).

Thus, to in depth define the pattern of cytokines modulated by hMENA^{11a}, we screened a panel of 40 cytokines/chemokines by a Bio-Plex assay in different NSCLC cell lines. H1650 cells produced high levels of different cytokines/chemokines, the highest being IL6. Importantly, the analysis of CM of si11a cells revealed a strong increase of IL6, IL8 and CXCL1 *vs* sictr H1650 cells (online supplemental figure S3C). We further confirmed

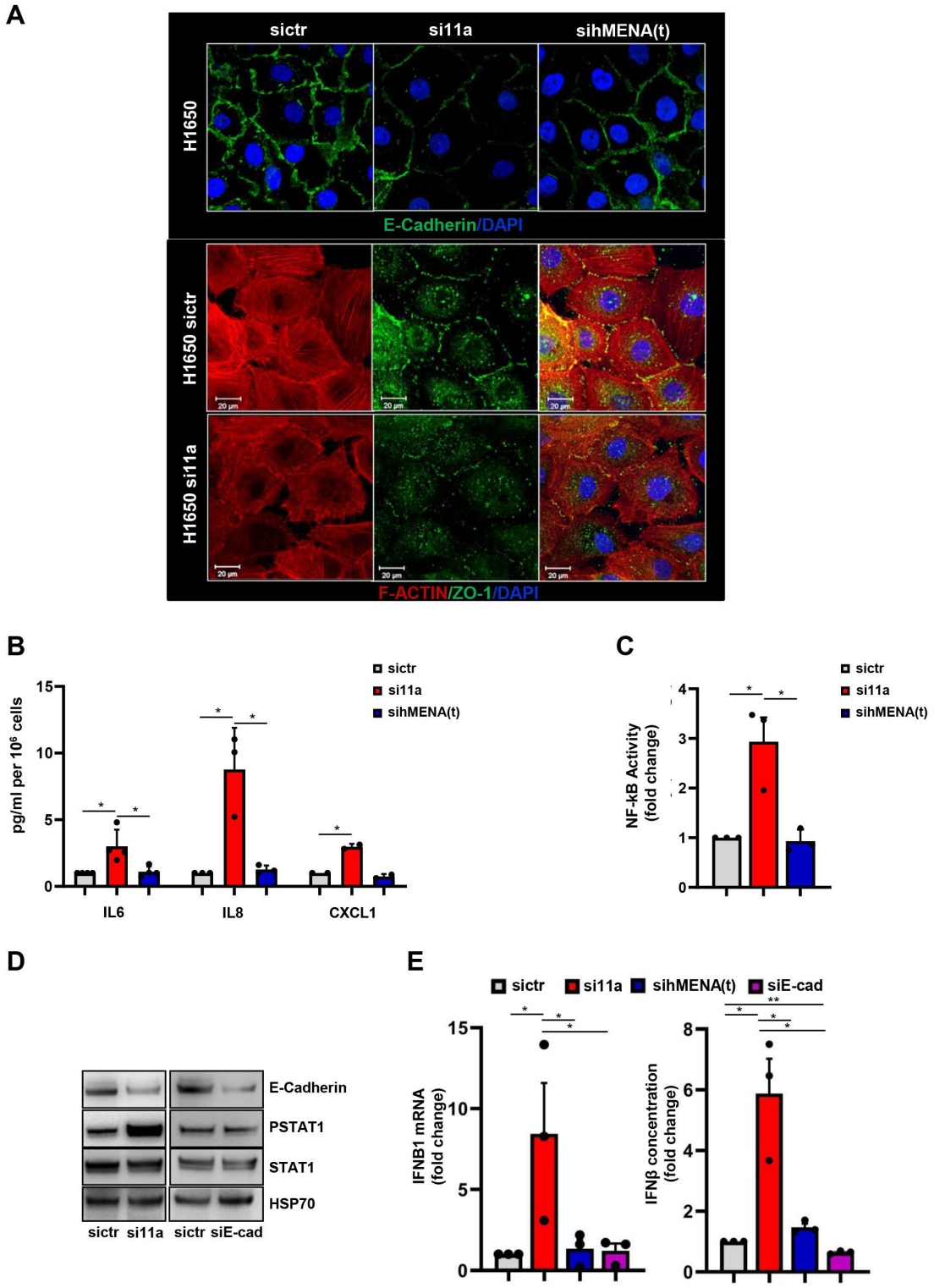

Figure 3 hMENA^{11a} depletion perturbs cell–cell junction, induces proinflammatory cytokines via NF-kB. E-cadherin loss does not activate IFN-I pathway. (A) Representative immunofluorescence images of sictr and si11a, sihMENA(t) H1650 cells stained with anti-E-Cadherin antibody (green) (upper panel) or with phalloidin (red) and anti-ZO-1 antibody (green) (lower panel). Nuclei were stained with DAPI. Scale bar: 20 µm. (B) ELISA for the indicated cytokines in supernatants of sictr, si11a and sihMENA(t) H1650 cells. (C) NF-kB transcriptional reporter activity was assessed by luciferase assays in sictr, si11a and sihMENA(t) H1650 cells. Cells were cotransfected with specific siRNAs and with inducible NF-kB responsive construct expressing Renilla luciferase. Forty-eight hours later, a luciferase assay was performed. (D) Western blotting of sictr, si11a and siE-Cadherin H1650 cells. Anti-HSP70 was used as loading control. (E) IFNβ expression at mRNA level (IFNB1, qRT-PCR, left) and protein level detected by ELISA in supernatants (right) of H1650 sictr, si11a, sihMENA(t) and siE-Cadherin cells. Graphs represent mean±SEM of three independent experiments. (B, C, E). P values were calculated by two-tailed Student's t-test. *P≤ 0.05; **P≤ 0.01.

by ELISA the increase of CXCL1, IL6 and IL8 levels in si11a cell-derived CM (figure 3B), compared with sictr and sihMENA(t) cells. Inflammatory cytokine regulation has been ascribed to NF-kB activity and accordingly we observed that hMENA^{11a} silencing induced a strong activation of NF-kB in H1650 cells, compared with sictr and sihMENA(t) cells as evidenced by luciferase assay (figure 3C).

Secretion of inflammatory cytokines and chemokines by si11a cells does not depend on cell senescence (senescence-associated secretory phenotype[32]). Long-term cultured cancer associated fibroblasts were used as senescence positive control (online supplemental figure S3D).

E-cadherin loss has been reported to be associated with NF-kB activation and inflammatory cytokine production.[30 33] To exclude that the pathways activated by hMENA^{11a} silencing are not related to its effects on E-cadherin down regulation, we analyzed the direct effects of E-cadherin depletion in H1650. As expected we found that levels of mRNAs of the two NF-kB target genes, IL6 and IL8, were increased in H1650 cells depleted of E-cadherin compared with sictr cells (online supplemental figure S3E), but notably we observed that STAT1 phosphorylation at Tyr 701 is not affected by E-cadherin silencing in H1650 cells (figure 3D). More importantly, IFNβ levels were unchanged in E-cadherin depleted cells (figure 3E).

These data evidence that hMENA^{11a} depletion perturbs cell–cell junction integrity, activates NF-kB pathway, induces proinflammatory cytokines but differently from E-cadherin loss specifically activates Type I IFN pathway, indicating that this effect is not related to cell–cell junction deregulation but likely to actin cytoskeleton disturbance occurring in the absence of hMENA^{11a}.

hMENA^{11a} depletion induces an increase of RIG-I which sustains STAT1 activation, PD-L1 upregulation and IFNβ secretion

Then, since Type I IFN production is activated by nucleic acid sensors,[34] we focused on the pattern recognition receptor RIG-I,[35] associated with the actin cytoskeleton and reported as colocalized with ZO-1, which is fundamental for its localization and activation for innate immune signaling. On cytoskeleton rearrangements, RIG-I delocalizes and activates type I interferon.[27]

We observed that hMENA^{11a} silencing, along with a critically disorganization of F-actin, induced an important delocalization of ZO-1 at cell junctions (figure 3A, lower panel). We hypothesized a role for RIG-I in IFN signaling activation observed in hMENA^{11a} silenced cells, also indicated by increased *DDX58* (RIG-I) transcript levels in si11a cell lines, compared with relative sictr cells (figure 1D). Furthermore, RIG-I expression also increases at protein level in all the si11a cell lines, compared with sictr cells (figure 4A,B and online supplemental figure S4A). It is important to note that, differently from hMENA^{11a}, E-cadherin silencing does not increase RIG-I levels (online supplemental figure S4B), indicating that a mechanism specifically related to actin dynamics, rather than cell junction integrity, may account for RIG-I signaling regulation.

To determine whether RIG-I has a role in sustaining IFN activation downstream to hMENA^{11a} silencing, we first analyzed the effects of RIG depletion in our cell lines (figure 4A,B), then, to demonstrate that RIG-I signaling is functional in our cells, we treated cells with M8, RIG-I agonist,[36] that, as expected, increased RIG-I levels and induced STAT1 activation (online supplemental figure S4C). We observed that si-RIG-I *per se* does not affect STAT1 expression and phosphorylation (figure 4A,B, online supplemental figure S4D and E). Differently, when we presilenced cells for RIG-I and then, 24 hours later, silenced also for hMENA^{11a}, we inhibited STAT1 phosphorylation, IFNβ and PD-L1 increase, indicating that RIG-I is crucial in sustaining the STAT1 pathway activation we identified in si11a cells (figure 4A,B, online supplemental figure S4D and E). Collectively these data indicate, in a panel of NSCLC cell lines, independently of their genomic alterations, that hMENA^{11a} regulates STAT1 activation, PD-L1 upregulation and IFNβ secretion *via* RIG-I.

IFNβ derived from si11a cells induces a unique macrophage phenotype and a paracrine loop which favors an EMT phenotype

Tumor cell intrinsic modifications may result in distinct immune responses, with macrophages being one of the key orchestrators of the TME. Type I IFN signaling activation characterizes a peculiar macrophage subtype, IFN-tumor-associated macrophage (TAMs), identified in different patients with cancer, including patients with lung cancer.[37] We then reasoned that the secretoma and the signaling pathways activated by hMENA^{11a} downregulation may influence macrophage polarization. Thus, we treated human monocyte-derived M0 macrophages (MΦs) for 24 hours with the CM collected from sictr, si11a and sihMENA(t) H1650 cells. The exposure of MΦs to tumor CM induced a M2-like phenotype, as shown by the modulation of typical M2-like markers, such as CD163, CD206 and IL10 (figure 5A,B and online supplemental figure S5A) and their morphology (online supplemental figure S5B).[38] Notably, macrophages treated with CM-si11a (thereafter si11a-MΦs) exhibited a unique phenotype compared with CM-sictr and CM-siMENA-polarized MΦs, with high levels of CD16, HLA-DR and CD163 and low level of CD206 receptor but also higher expression of the M1-like costimulatory molecules CD80 and CD86, (figure 5A,B and online supplemental figure S5A). Interestingly, we found higher levels of PD-L1 and PD-L2 in si11a-MΦs with respect to sictr and siMENA-MΦs and increased levels of IL10 and TGFβ cytokines (figure 5A,B and online supplemental figure S5A).

Considering that IFNβ has been reported to upregulate CD80 and CD86[39 40] as well as IL10,[41] we hypothesized

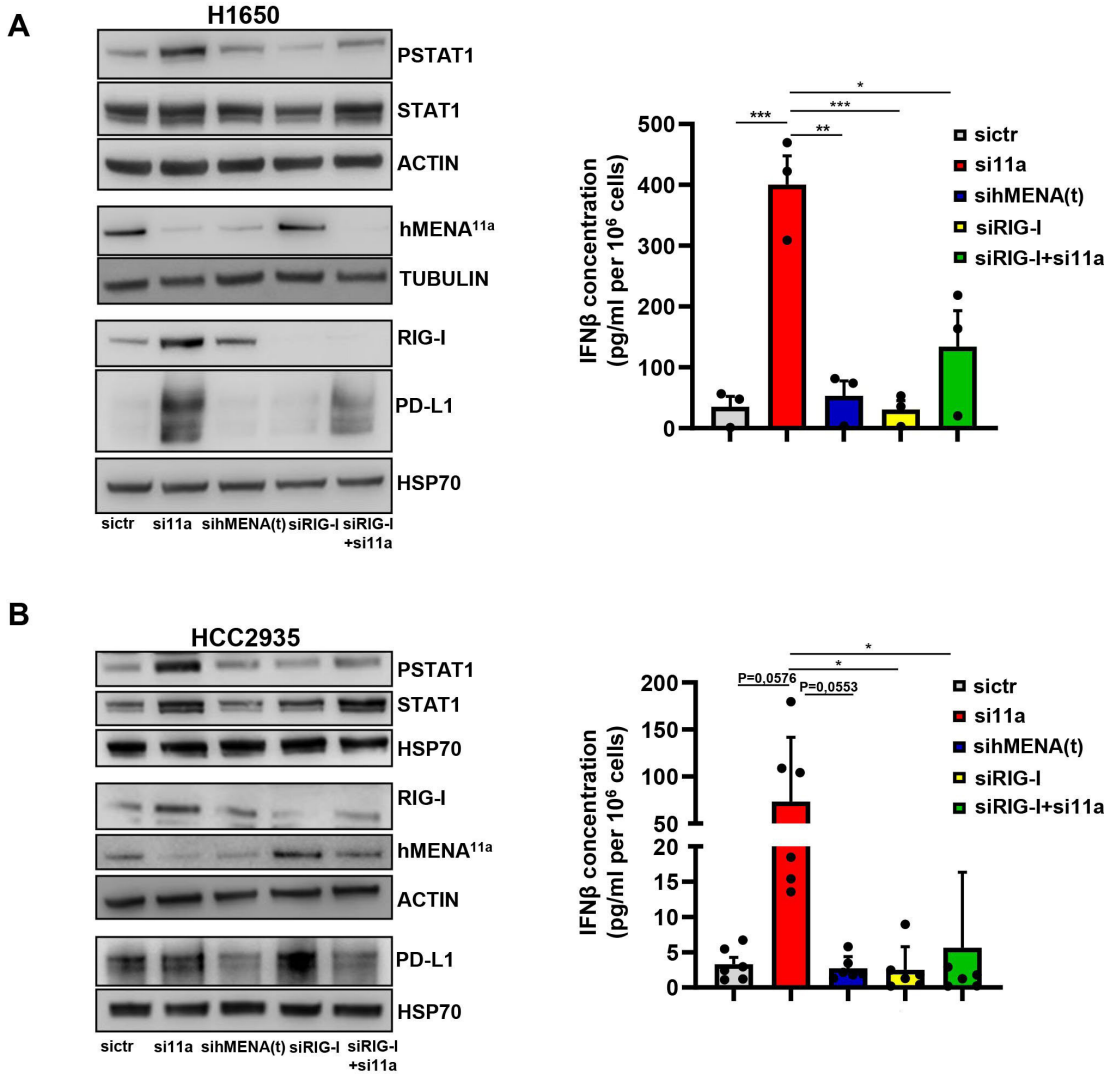

Figure 4 hMENA^{11a} depletion induces an increase of RIG-I which sustains IFNβ production, STAT1 activation and PD-L1 upregulation. (A, B) (*Left*) Western blotting analysis of sictr, si11a and sihMENA(t), siRIG-I and siRIG-I+si11a H1650 (A) and HCC2935 (B) cells. Anti-HSP70 was used as loading control. (A, B) (Right) IFNβ levels were measured by ELISA in supernatants of H1650 (A) and HCC2935 (B). Graphs represent the mean±SEM of three independent experiments. (A, B) P values were calculated by two-tailed Student's t-test.

that IFNβ, found at high levels in CM-si11a, may have a role in this unique MΦ polarization.

IFNβ treatment (24 hours) on monocyte-derived M0-macrophages determined a MΦ polarization status that significantly resembles the phenotype observed after CM-si11a exposure (online supplemental figure S5D). To investigate whether IFNβ signaling is required for the CM-si11a-mediated polarization of MΦs, we blocked IFN-αβ-receptor (IFNAR) for 48 hours with anti-IFNAR Chain 2 Antibody (figure 5C and online supplemental figure S5C). Noteworthy, the upregulation of IL10, TGFβ, PD-L1 and PD-L2 is abrogated in si11a-MΦs. Conversely, we observed that IFNAR blockade counteracts the CM-si11a-mediated CD206 downregulation (figure 5C). Overall, secretome of hMENA^{11a} depleted cancer cells, via IFNβ signaling, forces the macrophages toward a peculiar polarization, characterized by co-expression of both M1-like and M2-like markers.

To identify whether hMENA^{11a} loss activates a paracrine loop between tumor cells and macrophages, favoring an EMT phenotype in cancer cells, we treated A549 cells with CM derived from macrophages cultured with tumor supernatants (CM-TUM/MΦ-s). Interestingly, tumor cells treated with CM-TUM/MΦ-si11a expressed higher levels of the EMT marker vimentin, compared with cells cultured with CM-TUM/MΦ-sictr, indicating that soluble mediators produced by macrophages polarized by cancer cells depleted of hMENA^{11a} can favor EMT of the surrounding cells, likely affecting tumor cell invasiveness (figure 5D).

These data indicate that the secretoma and signaling pathways activated by hMENA^{11a} downregulation activates a paracrine loop resulting in a peculiar polarization of macrophages that favors an EMT phenotype in cancer cells.

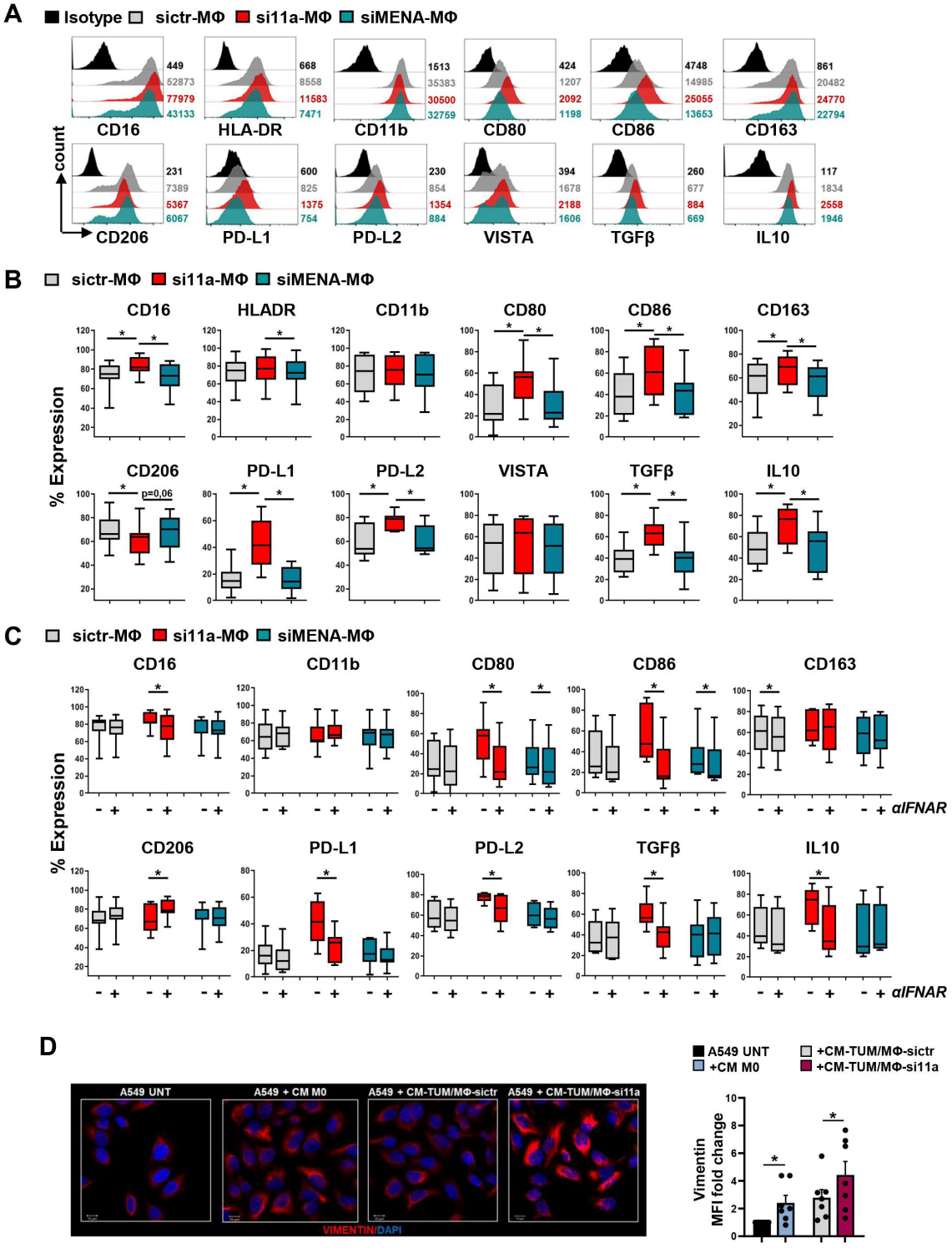

Figure 5 Conditioned medium derived from si11a NSCLC cells induces a unique macrophage phenotype. (A) Mean fluorescence intensity (MFI) expression levels of macrophage-specific markers shown in a representative flow cytometry analysis. Monocyte-derived M0-MΦs from healthy donors (HDs) were polarized for 24 hours with CM derived from sictr, si11a and sihMENA(t) H1650 cells (sictr-MΦs, si11a-MΦs, siMENA-MΦs, respectively). MFI values are indicated. (B) Levels of expression of macrophage markers by flow cytometry in MΦs treated as in (A) (n=9). Median value, first and third quartiles by box, minimum and maximum by whiskers. (C) Analysis of expression levels of selected macrophage markers by flow cytometry in M0-MΦs untreated or treated for 48 hours with anti-IFNAR Chain 2 Antibody (1 µg/mL), and then polarized with CM from sictr, si11a and sihMENA(t) H1650 cells (n=7). (D) (Left) Representative images of immunofluorescence analysis of A549 cells untreated (UNT) or treated with CM from M0-MΦs, CM-TUM/MΦ-sictr or CM-TUM/MΦ-si11a, stained with anti-Vimentin antibody (red). Nuclei were stained with DAPI. Scale bar: 20 µm. (Right) Quantitative analysis of Vimentin levels. MFI of vimentin/DAPI of three different fields per sample were reported as fold changes (n=7). P values were calculated by Wilcoxon rank test, with Bonferroni correction for multiple comparison. *p≤0.05. NSCLC, non-small cell lung cancer.

hMENA^{11a} expression, IFN and macrophage scores stratify GR or PR ICB-treated NSCLC patients

To translate our experimental findings into the clinical setting, we profiled tumor tissues of 15 NSCLC patients treated with ICB therapy (nivolumab or pembrolizumab) by Nanostring nCounter PanCancer IO 360 Panel, integrated with custom probes for hMENA splicing variants. We compared the gene expression profile of seven patients classified as PRs, with eight patients classified as GRs.

The differential gene expression analysis between GR and PR patients evidenced that 318 genes were modulated in the two groups (58 genes upregulated and 260 downregulated in GRs *vs* PRs) (online supplemental file 2). In line with our previous data on the role of hMENA^{11a} as prognostic factor in NSCLC, we found that hMENA^{11a} transcripts (ENAHa) were downregulated in PR patients, suggesting that low expression of hMENA^{11a} identify patients with poor response to ICB. In line with our experimental results, genes belonging to the Type I IFN pathway, namely IRF1, IRF2, STAT1, OASL, were upregulated in PR patients (figure 6A), again supporting that hMENA^{11a} loss activates IFN signaling pathway. Noteworthy, we found statistically significant higher levels of 'IFN Response Signature' included in IO 360 Panel in PRs than GRs (figure 6B, upper panel, left), indicating that IFN-related gene expression correlates with poor clinical response to checkpoint therapy in our patient setting. This was confirmed by the analysis of 'Interferon Response' module expression, recently identified among recurring gene modules across diverse cancer types[42] (figure 6B). Notably, we observed that this module is more expressed in our PR patients, further supporting that interferon signaling may be linked to a poor prognosis. Considering our data on the paracrine-loop between cancer cells and macrophages, we then analyzed the NanoString macrophage score (CD68, CD84, MS4A4A, CD163) in our patients and we observed an enrichment in PR patients as indicated in figure 6B, upper panel, left. Recently the IFN-TAM subset, resembling M1-like macrophages, but with immunosuppressive functions, has been reported.[37] Notably this gene signature was higher in our non-responder patients (figure 6B, upper panel, right), further supporting our experimental data (figure 5) and suggesting a crucial role of IFN-TAMs in ICB response in NSCLC patients. Then, to exclude the involvement of dendritic cells (DCs) as other immune cells related to ICB response mediated by hMENA^{11a} downregulation and Type I IFN activation, we looked at NanoString DC score (CCL13, CD209, HSD11B1) and, differently from macrophages, we did not evidence significant differences between GR and PR patients (online supplemental figure S7A).

To validate findings from our discovery cohort we evaluated the IFN and Macrophage gene signatures in two large cohorts of advanced NSCLC patients treated with ICB in second or third line, the OAK (NCT02008227)[43] and POPLAR (NCT01903993)[44] datasets. Since the expression levels for transcript variants are not available in these datasets, we used ESRP1, the splicing regulator of 11a exon inclusion, and ENAH gene expressions as proxy to estimate hMENA^{11a} expression[45] after validating its robustness on TCGA Lung data as shown in online supplemental methods and figure S6. Notably, we were able to confirm that patients classified as having low expression of the hMENA^{11a} transcript and showing poor response exhibited elevated levels of both IFN and Macrophages gene signatures (figure 6C).

A mechanistic link sustaining tumor immune evasion has been reported between TAM abundance and CD8$^+$ T cell exhaustion, on prolonged residence in the TME.[46] Thus, we have looked at CD8$^+$ T cells and CD8$^+$ exhausted cells in the three datasets of ICB-treated patients (online supplemental figure S7A–D). Of note, PRs (hMENA^{11a} low, Type I IFN high) in Nanostring cohort display a higher exhausted CD8$^+$ T cell score. This was confirmed also in validation cohorts (online supplemental figure S7D), suggesting that T cell exhaustion is linked to macrophage abundance, as recently reported.[46]

Similarly to our discovery cohort, DC abundance obtained by deconvolution analysis performed with two different computational tools, did not differ among GR and PR patients in OAK and POPLAR cohorts (online supplemental figure S7B,C).

Collectively these data strongly suggest that actin cytoskeleton modification related to hMENA^{11a} loss may influence the interferon response, activate a loop with macrophages, likely contributing to an immunosuppressive TME which hampers the response to ICB.

DISCUSSION

Growing evidence highlights that, among different biological processes, cellular cytoskeleton components and actin cytoskeleton dynamics may also modulate host immunity.[26 47 48]

We have previously demonstrated that the splicing of hMENA, which accompanies dramatic cytoskeleton modifications,[20] activates crucial pathways with an impact on patient prognosis.[22 23] However, no data are available on how actin cytoskeleton disturbance can contribute to both cancer cell intrinsic and extrinsic mechanisms involved in resistance to ICB.

Here, we delineate a novel role for the epithelial-associated hMENA^{11a} isoform, that when low expressed is able to modulate Type I IFN pathway, secretion of different inflammatory mediators, and IFNβ via the viral sensor RIG-I, regulating tumor PD-L1 expression in a panel of NSCLC cell lines, regardless of their molecular context. Moreover, we demonstrated that the secretome of tumor cells with low expression of hMENA^{11a} results in a macrophage peculiar polarization and activates a paracrine loop which favors EMT in cancer cells. Of clinical relevance we found that low hMENA^{11a} expression, high IFN and macrophage scores identify PRs among ICB-treated NSCLC patients.

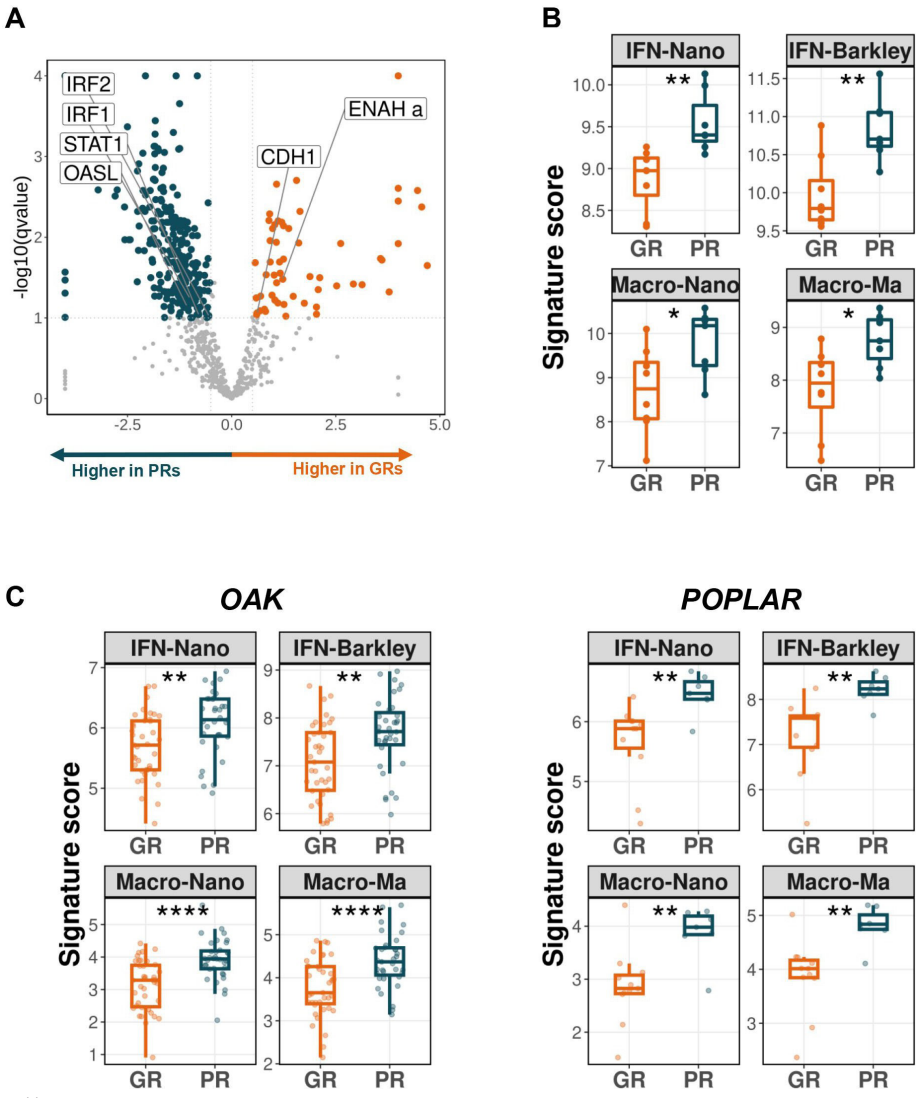

Figure 6 Low hMENA[11a] expression, high IFN pathway and Macrophage score identify poor responder ICB treated NSCLC patients. Differential Gene Expression Analysis (DGEA) between seven poor responders (PRs) and eight good responders (GRs) ICB treated NSCLC patients, by Nanostring nCounter PanCancer IO 360 Panel and custom probes for hMENA splicing variants (ENAHa for hMENA[11a]). (A) Volcano plot showing statistical significance (q value, –log10 scaled) *vs* Fold Change (log2 scaled) for genes differentially expressed in good responder cohort (GRs) *vs* poor responder cohort (PRs). Genes with –log10 (qvalue) <0.1 were considered significantly modulated. Log2 (Fold Change) positive values indicate higher expression in GRs (orange), log2 (Fold Changes) negative values indicate higher expression in PRs (blue). Selected genes are reported. The complete list of differentially expressed genes between GRs and PRs is reported in online supplemental file 2. (B) Boxplots showing the comparison of scores (log2 scaled) of four reported signatures between GRs and PRs in our internal cohort. IFN-Nano: IFN Response Signature Pathway included in IO 360 Panel by NanoString (t-test p<0.01); IFN-Barkley: Interferon Response Module reported by Barkley *et al*[42] (t-test p<0.01); Macro-Nano: Macrophage signature genes included in IO 360 Panel by NanoString (t-test p<0.05); Macro-Ma: signature genes of IFN-TAM cluster reported by Ma *et al*[37] (t-test p<0.05). (C) Boxplots showing the comparison of scores (log2 scaled) of the signatures reported in (B) between GRs and PRs in the OAK (39 *vs* 35 patients) and POPLAR (11 *vs* 7 patients) datasets. Shown in the boxplots are the medians (horizontal lines), 25th–75th percentiles (box outlines), and highest and lowest values within 1.5 times the interquartile range (vertical lines). T test OAK dataset: IFN-Nano: P=0.0024; IFN-Barkley: P=0.0021; Macro-Nano: P<0.00001; Macro-Ma: P<0.00001. T test POPLAR dataset: IFN-Nano: P=0.0035; IFN-Barkley: P=0.0025; Macro-Nano: P=0.003; Macro-Ma: P=0.0018. * P ≤ 0.05; ** P ≤ 0.01; **** P ≤ 0.0001. ICB, immune checkpoint blockade; NSCLC, non-small cell lung cancer.

Searching for mechanisms occurring when hMENA[11a] is depleted in NSCLC cell lines and underlying a viral mimicry with an upregulation of transcripts related to IFN pathways, we found the induction of IFNβ secretion and the activation of JAK/STAT1 pathway and in turn PD-L1 expression, ascribed to the increase of IRF-1 localization in the nucleus. This in accordance with the involvement of JAK/STAT1 pathway to an axis which includes IRF-1 and PD-L1[28] and in line with the findings that, after persistent IFN stimulation, STAT1 increases and sustains the expression of a subset of ISGs.[49] Although often associated with tumor-suppressive activities due to

its pro-apoptotic function, IRF1 is necessary for PD-L1 upregulation in tumor cells and sustains cancer progression in vivo, by inhibiting antitumor immunity.[50] Noteworthy, our ATAC-seq analysis identified an unknown regulatory region in PD-L1 promoter in hMENA^{11a} silenced cells. Although further studies are needed to identify transcription factors binding these regions, this data support the concept that hMENA-related actin cytoskeleton modifications link cytoarchitecture and gene activity, as we and others have suggested.[23 51] Indeed recently, it has been described that hMENA has a role in the nuclear membrane where controls the LINC (Linkers of the nucleoskeleton and cytoskeleton) complex, chromatin organization and cancer specific immune genes (ie, PTX3 and IL-1β).[51]

The perturbation of the epithelial barrier, as occurring when E-cadherin is lost, a primary event in the EMT program, results in NF-kB activation via an intrinsic mechanism not linked to infection and able to promote the secretion of inflammatory cytokines. EMT has been reported to be immunosuppressive in breast cancer.[16] Our results revealed that hMENA^{11a} depletion perturbs cell–cell junction integrity and downregulates E-cadherin, activates NF-kB pathway and promotes secretion of inflammatory cytokines and chemokines. However, differently from E-cadherin downregulation, hMENA^{11a} depletion also induces IFNβ production, resembling a sterile inflammation. The transcriptional induction of IFN-Is is mediated by the activation of (RIG-I)-like receptors (RLRs), key players in the recognition of viral RNA. The observation that RIG-I sustains IFNβ transcription and secretion in hMENA^{11a} silenced cells supports the hypothesis that hMENA^{11a}-related actin cytoskeleton disturbance may affect innate immunity. Likewise, in viral infections the actin cytoskeleton structure affects proper activation of antiviral response, by acting as tracks that direct RIG-I to mitochondria,[52] or by affecting the activation status of viral signaling components.[26] Similarly, in cancer RIG-I has been reported to associate with actin cytoskeleton in epithelial cancer cells, where actin depolymerization is sufficient to induce RIG-I activation and in turn IFNβ production.[27] Although the mechanism involved in RIG-I activation after hMENA^{11a} loss has still to be clarified, we hypothesize that hMENA^{11a} depletion releases RIG-I from actin cytoskeleton, determining its activation. Further studies are needed to identify whether actin cytoskeleton disturbance mediated by hMENA^{11a} downregulation may activate nucleic acid sensors other than RIG-I. According to these data, diverse actin cytoskeleton related proteins have been reported as a scaffold for immune sensors. In mouse embryonic fibroblasts, focal adhesion kinase (FAK), key component of focal adhesions, linking extracellular matrix to actin cytoskeleton, relocalizes from FAs to the mitochondrial membrane, where it colocalizes with MAVS, critical component of RIG-I antiviral signaling, potentiating MAVS-mediated antiviral signaling.[53] Noteworthy we have previously reported that tyrosine phosphorylation of FAK at Y397, determinant of FAK localization,[54] is affected by hMENA isoform expression in breast cancer cells.[23]

Although numerous studies have reported a tumor suppressive role of RIG-I, there is a growing body of evidence in favor of its protumor behavior, evidencing a context-dependent function of RIG-I.[55 56] Wolf *et al* report a correlation of RIG-I expression with poor ovarian cancer survival and found that tumors with high RIG-I expression were markedly enriched in PD-L1 and FoxP3 expression, suggestive of a RIG-I-related immunosuppressive TME.[55] The activation of RIG signaling in breast cancer cells, mediated by activated stromal cells has been linked to tumor growth, metastasis, and therapy resistance.[56]

Although the role of macrophages in tumors has been extensively explored and inflammatory IFN-I signaling promotes macrophage maturation and stimulatory capacity,[57] the negative impact of IFN-I is less well understood. Our data reveal that the secretome and activated signaling pathways related to hMENA^{11a} downregulation are able to polarize macrophages (si11a-MΦ), toward a peculiar phenotype. We can speculate that this peculiar phenotype of macrophages may resemble IFN-TAMs, one of the functional TAM subsets identified across many tumor types, including NSCLC, and characterized by the high expression of IFN-regulated genes, including CD86 and immune checkpoint molecules, such as PD-L1.[37] Noteworthy, in our experimental settings, blocking macrophage IFN receptor impedes the increase of PD-L1 and CD86 levels observed when macrophages are treated with si11a-derived CM, supporting the critical role of IFNβ in dictating the peculiar macrophage phenotype. The attempts to relate macrophage phenotype to function have evidenced the importance of various external cues derived from the heterogeneous TME, including signals from neighbor cancer cells, in determining TAM functional diversity.[37]

Noteworthy, IFN-TAMs, although resembling M1-like macrophages, have been associated to immune suppressive functions by different studies.[37]

Of relevance, we demonstrated that our conditioned si11a-MΦs are able to induce an increase of vimentin expression in tumor cells, indicating that this macrophage subtype may favor EMT in neighboring tumor cells as recently highlighted.[58] These data suggest that cancer-related actin modification and in turn IFNβ production induce a protumor behavior in macrophages. Of clinical relevance, Nanostring analysis on tumor tissues of NSCLC patients classified as PRs or GRs based on their response to ICB, revealed higher expression of hMENA^{11a} in GR patients, characterized by low expression of several IFN-I related genes. Notably computed IFN score as well as macrophage score was higher in PRs, while DC score was similar in GRs and PRs. Of note, an increase of exhausted CD8 was found in PRs, in agreement with recent findings highlighting the link of TAM and exhausted CD8 T cells in the TME.[46]The validation of these data in two large clinical studies (OAK and POPLAR) paves the way for the likelihood of considering these associated molecular

signatures as a hallmark of a TME subtype related to resistance to ICB, although further studies are needed to support these findings and their clinical translation toward precision immuno-oncology.

Taken together, our data imply that the hMENA^{11a}-mediated IFNβ signaling and secretion sustain an immune suppressive TME and likely represent a mechanism of resistance to ICB-based therapy.

This detrimental, rather than beneficial effect of intratumoral IFN signature, is still largely debated. Recently, it has been attributed to chronic Type I IFN signaling that we could speculate may occur when disturbance of cytoskeleton related to hMENA^{11a} downregulation activates a chronic inflammation. As soon as more datasets of ICB-treated patients will be available also in early clinical setting, they throw light on the effects of actin cytoskeleton and type I IFN activation, bringing to the forefront the possibility of novel robust signatures to stratify ICB responder or not responder patients.

Author affiliations
[1]Tumor of Immunology and Immunotherapy Unit, IRCCS Regina Elena National Cancer Institute, Rome, Italy
[2]Institute of Biochemistry and Cell Biology, Consiglio Nazionale delle Ricerche, Rome, Italy
[3]Department of Biosciences, School of Science and Technology, Nottingham Trent University, Nottingham, UK
[4]SAFU Unit, IRCCS Regina Elena National Cancer Institute, Rome, Italy
[5]NanoString Technologies Inc, Seattle, Washington, USA
[6]Biostatistics Unit, IRCSS Regina Elena National Cancer Institute, Rome, Italy
[7]Pathology Unit, IRCCS Regina Elena National Cancer Institute, Rome, Italy
[8]Second Division of Medical Oncology, IRCCS Regina Elena National Cancer Institute, Rome, Italy
[9]Department of Oncology, IRCCS Ospedale San Raffaele, Milan, Italy
[10]Department of Health Sciences, Human Pathology Section, Tumor Immunology Unit, University of Palermo, Palermo, Italy
[11]Department of Oncology, IRCCS Humanitas Research Hospital, Rozzano, Milan, Italy
[12]Department of Immunology and Inflammation, IRCCS Humanitas Research Hospital, Rozzano, Milan, Italy
[13]Department of Medical Biotechnology and Translational Medicine, University of Milan, Milan, Italy

Acknowledgements We thank all patients who donated samples for this study. We thank Prof Sandra De Maria for her fruitful, constructive advice, Prof John Hiscott for kindly providing the RIG-I agonist M8 and Dr Roberta Melchionna for helpful scientific discussions. We thank Maria Vincenza Sarcone, Annalisa Antonini and Giuliana Falasca for technical assistance. This research makes use of Data generated by Genentech. Graphic abstract was created with BioRender (http://biorender.com/).

Contributors PT and PN conceived the study. PT and AT performed most of the experiments. BP and AT performed macrophages and flow cytometry experiments; ADC performed qRT-PCR assays; FDM performed confocal microscopy; LD'A and DD'A designed and conducted bioinformatics analyses, and critically interpreted the results; FDN and FG performed RNA seq, ATAC-Seq and Nanostring gene expression assays; GC analyzed ATAC-Seq data sets; FP performed and analyzed Bioplex assay; MP provided technical support; IS performed statistical analysis; SB contributed to siRNA experiments; PV provided pathological review of patient tissues; SC, FC, VR, PAZ and VG managed NSCLC patients and provided clinical data; FM and CT provided expert feedback; PT, PN and AT wrote the manuscript; all authors read and approved the manuscript. PN acts as guarantor.

Funding This work was supported by AIRC IG No 19822. This study was funded by the Italian Ministry of Health under the aegis of Alliance Against Cancer RCR-2019-23669120. AT was supported by a AIRC fellowship for Italy 2021, project code 26875.

Competing interests None declared.

Patient consent for publication Not applicable.

Ethics approval The study was approved by Comitato Etico Centrale IRCSS Lazio: Studio 'ACC LUNG2' (Prot. Number 1152/18); AIRC IG: 'hMENA splicing in the dialogue between tumor, ECM, CAFs and immune cells: Role in NSCLC progression and drug resistance' (Prot. Number 1008/17). The informed consent was obtained from all the patients included in this study.

Provenance and peer review Not commissioned; externally peer reviewed.

Data availability statement Data are available in a public, open access repository. Data may be obtained from a third party and are not publicly available. All data generated or analyzed during this study are included in this article and its online supplemental information files. The datasets generated during the current study have been deposited in the Gene Expression Omnibus (GEO) under the following accession codes: ATAC-Seq dataset: GSE224246 (https://www.ncbi.nlm.nih.gov/geo/query/acc.cgi?&acc=GSE224246); RNA-Seq datasets: GSE224216 (https://www.ncbi.nlm.nih.gov/geo/query/acc.cgi?acc=GSE224216); GSE217451 (https://www.ncbi.nlm.nih.gov/geo/query/acc.cgi?acc=GSE217451). [OAK] and [POPLAR] datasets were obtained by Genentech as third part.

ORCID iDs
Lorenzo D'Ambrosio http://orcid.org/0000-0002-9656-7436
Sarah Warren http://orcid.org/0000-0002-5046-2890
Federica Marchesi http://orcid.org/0000-0002-7212-5721
Paola Nistico http://orcid.org/0000-0003-4409-2261

REFERENCES

1 Govindan R, Aggarwal C, Antonia SJ, *et al*. Society for Immunotherapy of cancer (SITC) clinical practice guideline on Immunotherapy for the treatment of lung cancer and Mesothelioma. *J Immunother Cancer* 2022;10:e003956.
2 Anagnostou V, Landon BV, Medina JE, *et al*. Translating the evolving molecular landscape of tumors to biomarkers of response for cancer Immunotherapy. *Sci Transl Med* 2022;14:eabo3958.
3 Parker BS, Rautela J, Hertzog PJ. Antitumour actions of Interferons: implications for cancer therapy. *Nat Rev Cancer* 2016;16:131–44.
4 Musella M, Guarracino A, Manduca N, *et al*. Type I Ifns promote cancer cell Stemness by triggering the epigenetic regulator Kdm1B. *Nat Immunol* 2022;23:1379–92.
5 Chen J, Cao Y, Markelc B, *et al*. Type I IFN protects cancer cells from Cd8+ T cell-mediated cytotoxicity after radiation. *J Clin Invest* 2019;129:4224–38.
6 Jain MD, Zhao H, Wang X, *et al*. Tumor interferon signaling and suppressive myeloid cells are associated with CAR T-cell failure in large B-cell lymphoma. *Blood* 2021;137:2621–33.
7 De Angelis C, Fu X, Cataldo ML, *et al*. Activation of the IFN signaling pathway is associated with resistance to Cdk4/6 inhibitors and immune Checkpoint activation in ER-positive breast cancer. *Clin Cancer Res* 2021;27:4939.
8 Gong K, Guo G, Panchani N, *et al*. EGFR inhibition triggers an adaptive response by Co-opting antiviral signaling pathways in lung cancer. *Nat Cancer* 2020;1:394–409.
9 Boukhaled GM, Harding S, Brooks DG. Opposing roles of type I Interferons in cancer immunity. *Annu Rev Pathol* 2021;16:167–98.
10 Benci JL, Xu B, Qiu Y, *et al*. Tumor interferon signaling regulates a Multigenic resistance program to immune Checkpoint blockade. *Cell* 2016;167:1540–54.

11 Cucolo L, Chen Q, Qiu J, *et al*. The interferon-stimulated gene Ripk1 regulates cancer cell intrinsic and Extrinsic resistance to immune Checkpoint blockade. *Immunity* 2022;55:671–85.
12 Jacquelot N, Yamazaki T, Roberti MP, *et al*. Sustained type I interferon signaling as a mechanism of resistance to PD-1 blockade. *Cell Res* 2019;29:846–61.
13 Nisticò P, Bissell MJ, Radisky DC. Epithelial-Mesenchymal transition: general principles and pathological relevance with special emphasis on the role of matrix Metalloproteinases. *Cold Spring Harb Perspect Biol* 2012;4:a011908.
14 Yilmaz M, Christofori G. EMT, the cytoskeleton, and cancer cell invasion. *Cancer Metastasis Rev* 2009;28:15–33.
15 Sistigu A, Di Modugno F, Manic G, *et al*. Deciphering the loop of epithelial-Mesenchymal transition, inflammatory Cytokines and cancer Immunoediting. *Cytokine Growth Factor Rev* 2017;36:67–77.
16 Dongre A, Rashidian M, Eaton EN, *et al*. Direct and indirect regulators of epithelial-Mesenchymal transition-mediated immunosuppression in breast Carcinomas. *Cancer Discov* 2021;11:1286–305.
17 Bradley RK, Anczuków O. RNA splicing dysregulation and the hallmarks of cancer. *Nat Rev Cancer* 2023;23:135–55.
18 Warzecha CC, Jiang P, Amirikian K, *et al*. An ESRP-regulated splicing programme is abrogated during the epithelial-Mesenchymal transition. *EMBO J* 2010;29:3286–300.
19 Gertler FB, Niebuhr K, Reinhard M, *et al*. Mena, a relative of VASP and Drosophila enabled, is implicated in the control of Microfilament Dynamics. *Cell* 1996;87:227–39.
20 Di Modugno F, Iapicca P, Boudreau A, *et al*. Splicing program of human MENA produces a previously Undescribed Isoform associated with invasive, Mesenchymal-like breast tumors. *Proc Natl Acad Sci U S A* 2012;109:19280–5.
21 Bria E, Di Modugno F, Sperduti I, *et al*. Prognostic impact of alternative splicing-derived hMENA Isoforms in Resected, node-negative, non-small-cell lung cancer. *Oncotarget* 2014;5:11054–63.
22 Melchionna R, Iapicca P, Di Modugno F, *et al*. The pattern of hMENA Isoforms is regulated by TGF-B1 in Pancreatic cancer and may predict patient outcome. *Oncoimmunology* 2016;5:e1221556.
23 Di Modugno F, Spada S, Palermo B, *et al*. hMENA Isoforms impact NSCLC patient outcome through fibronectin/B1 integrin axis. *Oncogene* 2018;37:5605–17.
24 Tauriello DVF, Sancho E, Batlle E. Overcoming TGFβ-mediated immune evasion in cancer. *Nat Rev Cancer* 2022;22:25–44.
25 Horiguchi K, Sakamoto K, Koinuma D, *et al*. TGF-B drives epithelial-Mesenchymal transition through Δef1-mediated downregulation of ESRP. *Oncogene* 2012;31:3190–201.
26 Acharya D, Reis R, Volcic M, *et al*. Actin cytoskeleton remodeling primes RIG-I-like receptor activation. *Cell* 2022;185:3588–602.
27 Mukherjee A, Morosky SA, Shen L, *et al*. Retinoic acid-induced Gene-1 (RIG-I) Associates with the actin cytoskeleton via caspase activation and recruitment domain-dependent interactions. *J Biol Chem* 2009;284:6486–94.
28 Garcia-Diaz A, Shin DS, Moreno BH, *et al*. Interferon receptor signaling pathways regulating PD-L1 and PD-L2 expression. *Cell Rep* 2017;19:1189–201.
29 Dorand RD, Nthale J, Myers JT, *et al*. Cdk5 disruption attenuates tumor PD-L1 expression and promotes antitumor immunity. *Science* 2016;353:399–403.
30 Kuphal S, Poser I, Jobin C, *et al*. Loss of E-Cadherin leads to upregulation of Nfkappab activity in malignant Melanoma. *Oncogene* 2004;23:8509–19.
31 Perez-Moreno M, Song W, Pasolli HA, *et al*. Loss of P120 Catenin and links to mitotic alterations, inflammation, and skin cancer. *Proc Natl Acad Sci U S A* 2008;105:15399–404.
32 Campisi J. Aging, cellular Senescence, and cancer. *Annu Rev Physiol* 2013;75:685–705.
33 Stodden GR, Lindberg ME, King ML, *et al*. Loss of Cdh1 and Trp53 in the uterus induces chronic inflammation with modification of tumor Microenvironment. *Oncogene* 2015;34:2471–82.
34 Schlee M, Hartmann G. Discriminating self from non-self in nucleic acid sensing. *Nat Rev Immunol* 2016;16:566–80.
35 Yoneyama M, Kikuchi M, Natsukawa T, *et al*. The RNA Helicase RIG-I has an essential function in double-stranded RNA-induced innate antiviral responses. *Nat Immunol* 2004;5:730–7.
36 Castiello L, Zevini A, Vulpis E, *et al*. An Optimized retinoic acid-inducible gene I agonist M8 induces Immunogenic cell death markers in human cancer cells and Dendritic cell activation. *Cancer Immunol Immunother* 2019;68:1479–92.
37 Ma R-Y, Black A, Qian B-Z. Macrophage diversity in cancer Revisited in the era of single-cell Omics. *Trends Immunol* 2022;43:546–63.
38 Donadon M, Torzilli G, Cortese N, *et al*. Macrophage morphology correlates with single-cell diversity and prognosis in colorectal liver metastasis. *J Exp Med* 2020;217:e20191847.
39 Marckmann S, Wiesemann E, Hilse R, *et al*. Interferon-beta up-regulates the expression of Co-stimulatory molecules Cd80, Cd86 and Cd40 on monocytes: significance for treatment of multiple sclerosis. *Clin Exp Immunol* 2004;138:499–506.
40 Bauvois B, Nguyen J, Tang R, *et al*. Types I and II Interferons Upregulate the Costimulatory Cd80 molecule in monocytes via interferon regulatory Factor-1. *Biochem Pharmacol* 2009;78:514–22.
41 McNab FW, Ewbank J, Howes A, *et al*. Type I IFN induces IL-10 production in an IL-27-independent manner and blocks responsiveness to IFN-Γ for production of IL-12 and bacterial killing in Mycobacterium tuberculosis-infected Macrophages. *J Immunol* 2014;193:3600–12.
42 Barkley D, Moncada R, Pour M, *et al*. Cancer cell States recur across tumor types and form specific interactions with the tumor Microenvironment. *Nat Genet* 2022;54:1192–201.
43 Rittmeyer A, Barlesi F, Waterkamp D, *et al*. Atezolizumab versus Docetaxel in patients with previously treated non-small-cell lung cancer (OAK): a phase 3, open-label, Multicentre randomised controlled trial. *Lancet* 2017;389:255–65.
44 Fehrenbacher L, Spira A, Ballinger M, *et al*. Atezolizumab versus Docetaxel for patients with previously treated non-small-cell lung cancer (POPLAR): a Multicentre, open-label, phase 2 randomised controlled trial. *Lancet* 2016;387:1837–46.
45 Wang W, Taufalele PV, Millet M, *et al*. Matrix stiffness regulates tumor cell Intravasation through expression and Esrp1-mediated alternative splicing of MENA. *Cell Rep* 2023;42:112338.
46 Kersten K, Hu KH, Combes AJ, *et al*. Spatiotemporal Co-dependency between Macrophages and exhausted $Cd8^+$ T cells in cancer. *Cancer Cell* 2022;40:624–38.
47 Mostowy S, Shenoy AR. The cytoskeleton in cell-autonomous immunity: structural determinants of host defence. *Nat Rev Immunol* 2015;15:559–73.
48 Tolar P. Cytoskeletal control of B cell responses to antigens. *Nat Rev Immunol* 2017;17:621–34.
49 Cheon H, Stark GR. Unphosphorylated Stat1 prolongs the expression of interferon-induced immune regulatory genes. *Proc Natl Acad Sci U S A* 2009;106:9373–8.
50 Shao L, Hou W, Scharping NE, *et al*. Irf1 inhibits antitumor immunity through the upregulation of PD-L1 in the tumor cell. *Cancer Immunol Res* 2019;7:1258–66.
51 Li Mow Chee F, Beernaert B, Griffith BGC, *et al*. Mena regulates the LINC complex to control actin–nuclear Lamina associations, Trans-nuclear membrane signalling and cancer gene expression. *Nat Commun* 2023;14:1602.
52 Ohman T, Rintahaka J, Kalkkinen N, *et al*. Actin and RIG-I/MAVS signaling components Translocate to mitochondria upon influenza A virus infection of human primary Macrophages. *J Immunol* 2009;182:5682–92.
53 Bozym RA, Delorme-Axford E, Harris K, *et al*. Focal adhesion kinase is a component of antiviral RIG-I-like receptor signaling. *Cell Host Microbe* 2012;11:153–66.
54 Hamadi A, Bouali M, Dontenwill M, *et al*. Regulation of focal adhesion Dynamics and disassembly by Phosphorylation of FAK at tyrosine 397. *J Cell Sci* 2005;118:4415–25.
55 Wolf D, Fiegl H, Zeimet AG, *et al*. High RIG-I expression in ovarian cancer Associates with an immune-escape signature and poor clinical outcome. *Int J Cancer* 2020;146:2007–18.
56 Nabet BY, Qiu Y, Shabason JE, *et al*. Exosome RNA Unshielding couples Stromal activation to pattern recognition receptor signaling in cancer. *Cell* 2017;170:352–66.
57 Snell LM, McGaha TL, Brooks DG. Type I interferon in chronic virus infection and cancer. *Trends Immunol* 2017;38:542–57.
58 Casanova-Acebes M, Dalla E, Leader AM, *et al*. Tissue-resident Macrophages provide a pro-Tumorigenic niche to early NSCLC cells. *Nature* 2021;595:578–84.